Available online at www.sciencedirect.com

International Journal of Mass Spectrometry 271 (2008) 15–21

www.elsevier.com/locate/ijms

Dissociative electron attachment to nitromethane

E. Alizadeh, F. Ferreira da Silva [1], F. Zappa [2], A. Mauracher, M. Probst, S. Denifl, A. Bacher, T.D. Märk, P. Limão-Vieira [1], P. Scheier *

Institut für Ionenphysik und Angewandte Physik and Center of Molecular Biosciences Innsbruck, Universität Innsbruck, Technikerstr. 25, A-6020 Innsbruck, Austria

Received 13 September 2007; received in revised form 9 November 2007; accepted 13 November 2007
Available online 22 November 2007

Abstract

Dissociative electron attachment (DEA) measurements to nitromethane, CH_3NO_2, in the gas phase have been revisited by making use of a high mass-resolution sector field instrument. Anion efficiency curves for 16 negatively charged fragments have been measured in the electron energy region from about 0 to 16 eV with an energy resolution of ~1 eV. Eight new anions have been detected, $CH_2NO_2^-$, $CHNO_2^-$, CH_2NO^-, H_2NO^-, CH_3^-, CH_2^-, CH^- and H^-. The five most dominant product anions are NO_2^-, O^-, OH^-, CN^- and CNO^-, all of them featuring two high-energy resonances at about 5 eV and 10 eV. Formation of $CH_2NO_2^-$ at low electron energies has been explained in terms of DEA to highly vibrationally excited molecules. The standard enthalpy of formation of $CH_2NO_2^-$ and H^-, CH_2^- and NO^- radicals have been estimated as $\Delta_f H_g^\circ(CH_2NO_2^-) = -1.71$ eV, $\Delta_f H_g^\circ(H^-) = 2.09$ eV, $\Delta_f H_g^\circ(CH_2^-) = 3.5$ eV and $\Delta_f H_g^\circ(NO^-) = -1.93$ eV, respectively.
© 2007 Elsevier B.V. All rights reserved.

Keywords: Electron attachment; Cross-section; Nitromethane

1. Introduction

The electronic states spectroscopy and reaction dynamics of low-energy electron interactions with nitromethane, CH_3NO_2, have been extensively studied [1–4] (and references therein). These studies have been motivated due to the fact that this molecule (i) plays a particular role in the chemistry of the earth's atmosphere (up to the stratosphere), (ii) is a simple organic-nitro compound with typical characteristics of explosives and propellants and (iii) forms dipole-bound as well as valence anions upon binding an extra electron [5–6]. Nitromethane can also be expected to act as a human carcinogenic agent and therefore is of biological relevance.

In a recent publication [4] we demonstrated that the dissociative electron attachment (DEA) reaction involves the formation of a transient negative ion that subsequently dissociates into thermodynamically accessible channels. With the sensitivity of this previous experiment performed at room temperature, with an electron energy resolution of the order of 140 meV seven anions were observed in the energy range from about 0 to 9.5 eV. In the case of OH^-, CN^-, and CNO^-, ion formation at very low electron energies (~0 eV) has been observed in contrast to other previous studies. The formation of OH^- and CNO^- at these low electron energies was explained in terms of DEA to vibrationally excited molecules.

In the present experiments we re-investigated the negative ion formation in nitromethane at low electron energies (0–16 eV). The uniform transmission of a sector field mass spectrometer for all masses is a big advantage compared to the quadrupole instrument utilized in Ref. [4]. Anions formed with initial kinetic energy that is released during the DEA reaction are recorded with reduced efficiency in the monochromator instruments since extraction fields for the anions are kept at a minimum value [7]. In contrast, a strong extraction field applied in the presently used Nier-type ion source minimizes discrimination of energetic fragments and leads to anion efficiency curves that resemble the true cross-section curves closely. Due to the high sensitivity of the presently used set-up eight additional fragments could be detected, i.e., $CH_2NO_2^-$, $CHNO_2^-$, CH_2NO^-, H_2NO^-, CH_3^-, CH_2^-, CH^- and H^-. For several anions we were able to assign and identify isotopomers containing ^{13}C, ^{15}N, ^{18}O or ^{17}O based

---

* Corresponding author. Fax: +43 512 507 2932.
E-mail address: Paul.Scheier@uibk.ac.at (P. Scheier).

[1] Permanent address: Atomic and Molecular Collisions Laboratory, CEFITEC, Departamento de Física, Universidade Nova de Lisboa, 2829-516 Caparica, Portugal.

[2] Universidade Estacio de Sá, Rio de Janeiro, Brazil.

1387-3806/$ – see front matter © 2007 Elsevier B.V. All rights reserved.
doi:10.1016/j.ijms.2007.11.004

on the identical cross-section shape as the main isotopomer and the ratio of the partial cross-sections.

2. Experimental set-up

A two-sector-field mass spectrometer equipped with a standard Nier-type ion source was utilized in the present study. A schematic view of the instrument is shown in Fig. 1. The electron beam was guided by a homogeneous magnetic field of about 20 mT. This field is sufficiently high to prevent extraction of electrons from the ion source. The electron current was set to 10 μA and this value was reached at an electron energy of about 4 eV. Thus the anion yield at lower electron energies is reduced compared to the partial cross-section of the anions. A liquid sample of nitromethane, purchased from Sigma–Aldrich with a stated purity of >99%, was used for the present DEA measurements. The sample was degased by a repeated freeze–pump–thaw cycle prior to the experiments. An effusive molecular beam (diameter of the orifice of the capillary was 1 mm) was crossed at an angle of 60° with an electron beam. SF_6 was used as a calibrant for the electron energy scale and the electron energy resolution, indicating for the present experiments (hot cathode filament electron source) an energy resolution of ∼1 eV. The anions were pushed by a repeller lens out of the interaction region and accelerated by a voltage drop of 5 kV to the analyzing section of the mass spectrometer. After mass selection in the magnetic sector field the ions pass a 1.4 m long field-free region and enter the electrostatic sector field. For the present investigation the mass resolution was kept at a minimum value of about $m/\Delta m = 1000$ by open all slits to their maximum. The anions are detected with a channel electron multiplier from Dr. Sjuts Optotechnik GmbH operated in a pulse counting mode. The dynamic range of the instrument is more than seven orders of magnitude. Mass spectra were taken at different electron energies and for all anions, identified as products of DEA to nitromethane, anion efficiency curves from 0 to 16 eV were measured. Absolute cross-section values were obtained via normalization of the presently determined anion efficiency curves at electron energies above 4 eV to the cross-section values published previously by Sailer et al. [4]. A single normalization value was determined that results in the best agreement between all commonly measured anions.

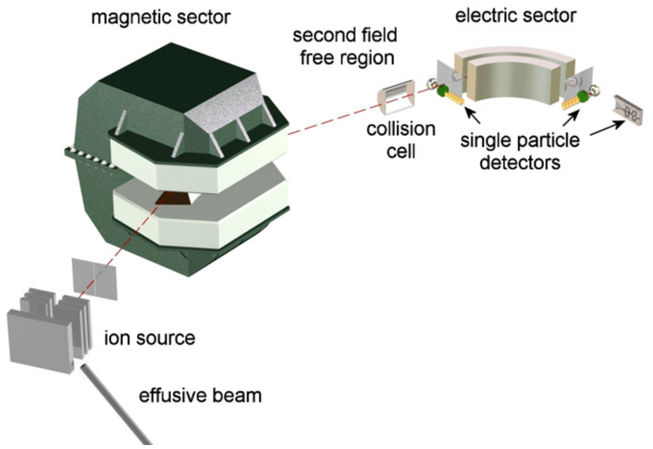

Fig. 1. Schematic view of the experimental set-up.

3. Computational section

For a better understanding of the experimental results high-level G3MP2 ab initio calculations have been carried out to obtain data on the energetics of nitromethane and the observed fragment anions. This is an extrapolation method that uses the results from several quantum chemical calculations in order to extrapolate towards molecular energies that would be obtained if complete inclusion of correlation energies and an unlimited basis set were possible. In general, the accuracy of G3(MP2) energies is in the order of about ±0.1 eV. For all of these calculations the Gaussian 03 program has been used.

4. Results and discussion

Fig. 2 shows negative ion mass spectra measured at three different electron energies, i.e., 0.7, 5 and 7 eV. A logarithmic scale was chosen for the anion yield to allow to see low intensity anions as well as the dominant fragments NO_2^- and O^-. At 0.7 eV the mass spectrum only shows NO_2^- which has its highest cross-section at this electron energy. The anions with a mass of 47 and 48 Da have 0.5% and 0.4% of the yield of NO_2^- which fits perfectly with the calculated isotopic pattern of the nitro isotopomer group. All other fragments such as CN^- and CNO^- are more than an order of magnitude less abundant. In contrast to the 0.7 eV mass spectrum the mass spectra at 5 eV and 7 eV show more than 30 fragments.

Figs. 3–6 show the electron energy dependences of the partial cross sections for DEA of 16 different fragment anions. As far as energy resolution is concerned, it plays a crucial role for the

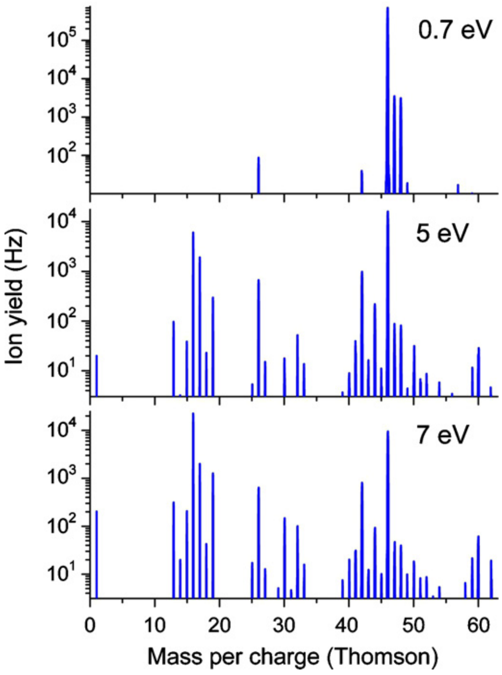

Fig. 2. Negative ion mass spectra measured at 0.7, 5 and 7 eV electron energies.

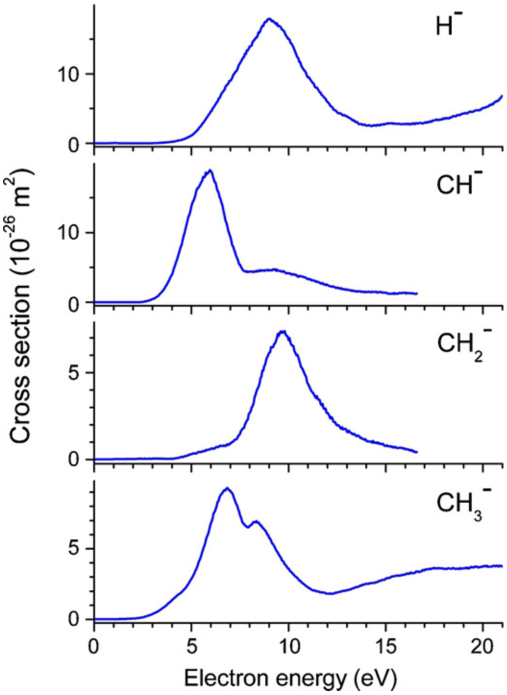

Fig. 3. Ion yields of H^-, CH^-, $CH_2{}^-$ and $CH_3{}^-$ from nitromethane as a function of the electron energy.

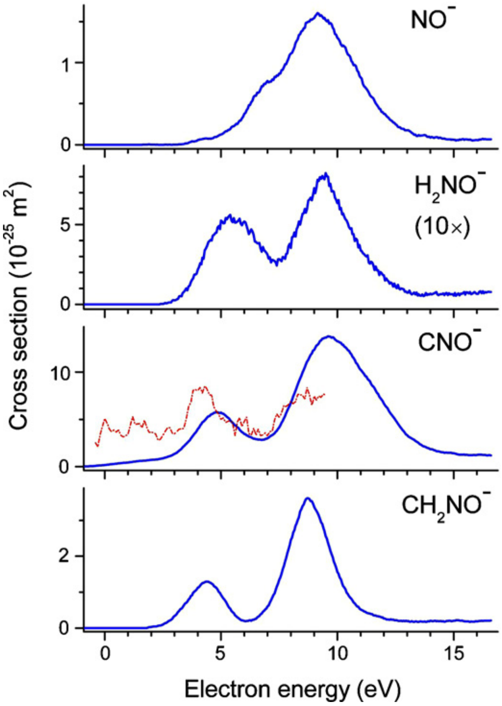

Fig. 5. Ion yields of NO^-, H_2NO^-, CNO^- and CH_2NO^- from nitromethane as a function of the electron energy. The dashed line represents cross-section data from Ref. [4].

shape of the low energy resonances (<4 eV), but is not so relevant for the high-energy region due to the broad nature of the observed features. Despite the high sensitivity of the presently utilized instrument, we were not able to detect any undissociated parent anion. A tiny signal at $m/z = 61$ could be assigned to an isotopomer of the dehydrogenated parent anion (see also Fig. 6 and Table 1), i.e., $^{13}CH_2NO_2{}^-$ which is too low in intensity to be seen in Fig. 2. The missing parent anion is also in agreement with our calculations showing that the electron affinity (EA) of this molecule is only 0.15 ± 0.10 eV. For the optimized geometry (at the level of MP2(Full)/6-31G(d) perturbation

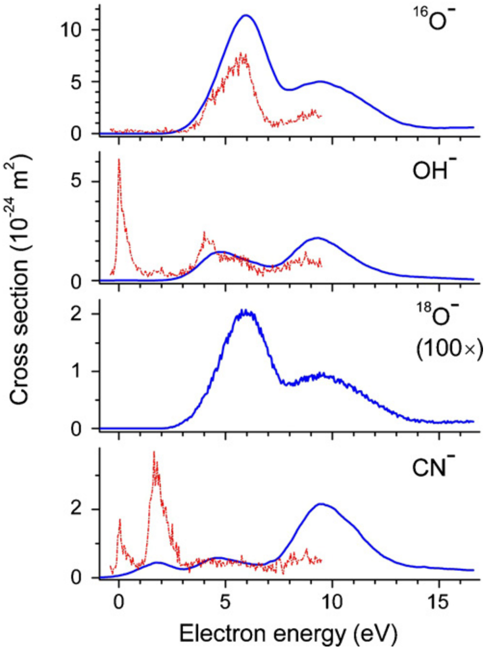

Fig. 4. Ion yields of $^{16}O^-$, OH^-, $^{18}O^-$ and CN^- from nitromethane as a function of the electron energy. The dashed lines represent cross-section data from Ref. [4].

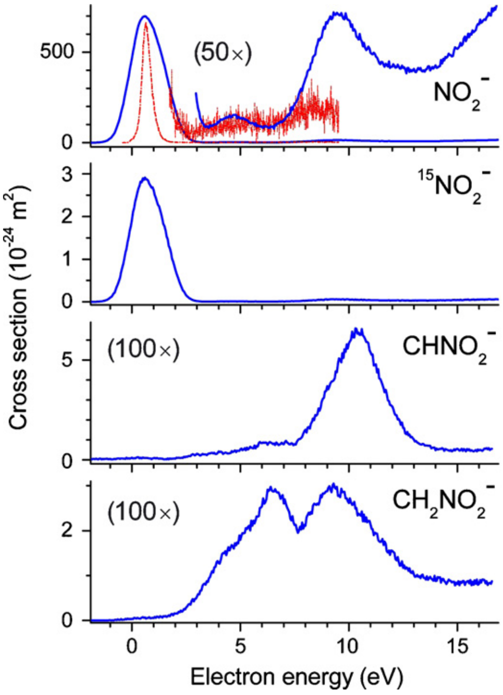

Fig. 6. Ion yields of $NO_2{}^-$, $^{15}NO_2{}^-$, $CHNO_2{}^-$ and $CH_2NO_2{}^-$ from nitromethane as a function of the electron energy. The dashed lines represent cross-section data from Ref. [4].

Table 1
Peak positions for the fragment ions obtained in the present experiment and reported in previous studies

Mass (Da)	Anionic species	Peak position in eV													
		Sailer et al. [4]						Present work							
60	$CH_2NO_2^-$	–	–	–	–	–	–	~0.5–	–	4	6.5	–	11	–	–
59	$CHNO_2^-$	–	–	–	–	–	–	–	–	4	6.5	–	10.5	–	–
47	$^{15}NO_2^-$	–	–	–	–	–	–	~0.5	–	–	–	–	9.5	–	–
46	NO_2^-	0.62	–	4	–	–	8	~0.5	–	4.5	–	–	9.5	–	–
44	CH_2NO^-	–	–	–	–	–	–	–	–	4.5	–	–	9.5	–	–
42	CNO^-	0	1.7	4	5.6	–	8.5		1.5–	–	5	–	9.5	–	–
32	H_2NO^-	–	–	–	–	–	–	–	–	–	5.5	–	9.5	–	–
30	NO^-	–	–	–	–	–	–	–	–	4	5.5	7	9	–	–
26	CN^-	0	1.7	4	5.6	–	~8	1	2	–	5	–	9	–	–
18	$^{18}O^-$	–	–	–	–	–	–	–	–	–	6	9	10.5	–	–
17	OH^-	0	–	4	5.5	–	8.7	–	–	4.5	–	9	–	–	–
16	O^-	–	–	4.1	5.4	5.9	~9	–	–	–	6	9	10.5	–	–
15	CH_3^-	–	–	–	–	–	–	–	–	4	7	8.5	–	–	–
14	CH_2^-	–	–	–	–	–	–	–	–	–	6	–	9.5	13	–
13	CH^-	–	–	–	–	–	–	–	–	~4.5	6	–	9.5	–	–
1	H^-	–	–	–	–	–	–	–	–	–	–	7.5	9	13	15

theory and basis set) of the neutral molecule the nitro group and the carbon atom are in-plane. This is not the case for the optimized geometry of the negatively charged molecule. Here the two oxygen atoms are symmetrically moved out of this plane.

The negative ion states at higher energy (>4 eV) can be considered to be formed via core excited resonances, which means, transient anions with the extra electron bound to an electronically excited state of the neutral. Moreover, the energy features in the range 9–11 eV can also be associated to Rydberg excitations [3] while those in the range 5–6 eV (for NO^-, CN^-, O^-, CH^- and H^-) are correlated to the second ($^1B_1$, $\sigma\pi^*$) and third ($^1B_2$, $\pi\pi^*$) electronically excited states of neutral nitromethane [3].

Fig. 7 shows the NO_2^- partial and the total cross sections on a semi-log scale as a function of the electron energy. It can be seen that the latter is at least in the low energy regime mainly due to the contribution of the former fragment ion, which is the dominant anion produced in DEA experiments to nitromethane.

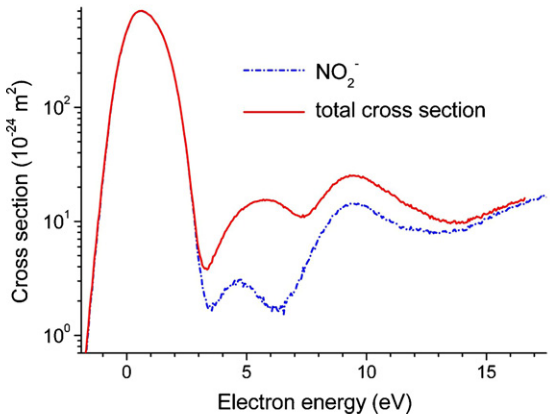

Fig. 7. NO_2^- partial and the total cross-sections on a semi-log scale from nitromethane as a function of the electron energy.

4.1. $CH_2NO_2^-$

The dehydrogenated closed shell anion $CH_2NO_2^-$ is formed via

$$e^- + CH_3NO_2 \rightarrow (CH_3NO_2)^{\#-} \rightarrow CH_2NO_2^- + H \qquad (1)$$

Reaction (1) represents a direct cleavage of the $H–H_2CNO_2$ bond in the transient anion with the negative charge remaining on the large fragment. The partial cross-section for the DEA reaction channel $CH_2NO_2^-/CH_3NO_2$ is shown in Fig. 6. The formation of the parent ion with H abstraction has been reported by Di Domenico and Franklin [1] exhibiting two resonances at 7.8 eV and a modest weak contribution at 0.6 eV, the position of the latter in good agreement with the present results (Fig. 6 and Table 1). The explanation, however given by those authors for the formation of this molecular ion is production through ion–molecule reactions, i.e., CH_3NO_2 reacting with O^-, with a resonance at 5.6 eV. This is in contradiction to the present observations from where we do not find any resemblance with the resonant structures between 4 and 8 eV. Moreover, our ionic yield measurements have been obtained with a pressure in the vacuum chamber of $\sim 10^{-4}$ Pa, therefore we exclude this assumption. It is clear that the shape of the O^- signal does not look like the shape of the $CH_2NO_2^-$ signal as would be expected in the case of ion-molecule reactions.

Reaction (1) is endothermic with a threshold at 1.95 eV as calculated from the bond energy $D(CH_2NO_2–H) = 4.40$ eV [8] and the electron affinity $EA(CH_2NO_2) = 2.45$ eV [9], therefore the formation of $CH_2NO_2^-$ ion at low electron energy around 0 eV is energetically not allowed. This is in good agreement with our calculations, where we estimated the bond energy to be $D(CH_2NO_2–H) = 4.43 \pm 0.10$ eV and the electron affinity to be $EA(CH_2NO_2) = 2.51 \pm 0.10$ eV. In the optimized geometry all atoms are in-plane, independent which hydrogen is lost. The experimental appearance energy of $CH_2NO_2^-$ is below this calculated threshold. This may indicate, as is the case for NO_2^-

production [4] and CH_3COO^- from acetic acid [10], that electron attachment proceeds through vibrationally excited states (hot bands) even though the number density of those modest hot molecules may be low. The high-energy resonances (Table 1) are certainly due to core-excited resonances.

4.2. $CHNO_2^-$

The low intensity cross-section of $CHNO_2^-/CH_3NO_2$ is shown in Fig. 6. Three resonances at 4, 6.5 and 10.5 eV (Table 1) can be assigned to electronically excited TNI states (including Rydberg excitation), which may then decompose via one anion fragment plus one H_2 neutral. $CHNO_2^-$ ion formation most probably proceeds through the following reaction

$$e^- + CH_3NO_2 \rightarrow (CH_3NO_2)^{\#-} \rightarrow CHNO_2^- + H_2 \qquad (2)$$

The value $\Delta_f H_g{}^\circ(H_2)$ is not known and therefore it is impossible to compute the thermodynamic threshold for a reaction (2) producing $CHNO_2^-$.

4.3. NO_2^- and $^{15}NO_2^-$

The present experiments yielding NO_2^- formation, by far the most intense of all fragments, are in good agreement with the previously reported in Ref. [4] but are observed here in the 8–16 eV energy region with better signal to noise ratio (see Fig. 6). The two resonances above 3 eV (Table 1) have been assigned to electronically excited TNI resonances (including Rydberg excitation), which may decompose via one anion fragment plus one or more neutrals. The NO_2^- cross-section increases above 13 eV suggesting ion pair formation. Taking into account the $AE(CH_3^+) = 13.6$ eV [12], and bearing in mind the present rather low energy resolution (~1 eV) such an assumption seems reasonable. It is interesting to note that the shape of the anion efficiency curves for NO_2^- measured with an electron monochromator instrument [4] and with the present Nier-type ion source is surprisingly similar. The height of the narrow resonance at 0.5 eV is expected to be significantly reduced when measured with a broad electron energy resolution. A possible explanation is reduced extraction efficiency of the monochromator instrument for fragment anions that are formed with some initial kinetic energy.

The partial cross-section for the DEA reaction channel $^{15}NO_2^-/CH_3NO_2$ is shown in Fig. 6, with one major resonance at 0.5 eV and a tiny contribution at 9.5 eV as observed for $^{14}NO_2^-$ (Table 1). The isotopic ratio ^{14}N:^{15}N of ~200:1 matches very well the observed intensities between the two isotopomers.

4.4. CH_2NO^-

This anion might be formed via the following two reactions:

$$e^- + CH_3NO_2 \rightarrow (CH_3NO_2)^{\#-} \rightarrow CH_2NO^- + OH \qquad (3a)$$

$$e^- + CH_3NO_2 \rightarrow (CH_3NO_2)^{\#-} \rightarrow CH_2NO_2{}^{\#-} + H \rightarrow CH_2NO^- + O + H \qquad (3b)$$

In Fig. 5 the relative cross-section for CH_2NO^- formation is shown. The shape and position of the resonance features for CH_2NO^-, CNO^- and H_2NO^- are very similar, which may indicate that these anions may have common precursor transient anion states. The appearance of a fragment ion with the composition of CH_2NO^- (reaction (3a)) is surprising due to the involvement of hydrogen transfer in the precursor ion and cleavage of an N–O bond (calculated bond energy $D(CH_3\text{–}NO_2) = 2.50 \pm 0.1$ eV). We can also assume for the reaction mechanism the suggested (3b) reaction of Di Domenico and Franklin [1]. Taking the $\Delta_f H_g{}^\circ(CH_3NO_2) = -0.841 \pm 0.001$ eV, $\Delta_f H_g{}^\circ(O) = 2.581 \pm 0.001$ eV [4] and the suggested $\Delta_f H_g{}^\circ(CH_2NO^-) \sim 0.16\text{–}0.31\ \mathrm{kJmol^{-1}}$ [8], we get an $AE(CH_2NO^-) \leq 3.73$ eV, where the equality holds for the case when reaction (3b) proceeds without excess energy (at the appearance energy). A close inspection of Fig. 5 reveals that the low energy resonance (centered at 4.5 eV) may have its threshold well below the calculated value, which may indicate that also for this anion attachment proceeds via vibrationally excited states.

The two resonances observed at 4.5 and 9.5 eV (Table 1) can also be assigned to electronically excited TNI states (including Rydberg excitation), which may decompose via one fragment anion plus one or more neutrals.

4.5. CNO^-

The formation of CNO^- in DEA has been reported before and the role of the TNI resonances as well as the different energetically favorable dissociation channels have been discussed in detail [4]. The present results in Fig. 5 reveal two broad features centered at 5 and 9.5 eV in accordance with the resonances at 5.6 and 8.5 eV, as reported by Sailer et al. [4].

4.6. H_2NO^-

Even though the intensity of this ion is quite low, it can tentatively arise from reaction

$$e^- + CH_3NO_2 \rightarrow (CH_3NO_2)^{\#-} \rightarrow H_2NO^- + CO + H \qquad (4)$$

where it might be associated with the C–N bond cleavage followed by rearrangement (hydrogen transfer) in the negative fragment into the stable configuration H_2NO^-. For the optimized geometry the two H atoms are out-of-plane with respect to N–O and the calculated electron affinity gives a value of 0.26 eV. Due to the presence of two resonances at 5.5 and 9.5 eV, the shape of the cross-section (Fig. 5) seems to indicate that the situation is similar as in the case of reaction (3a) and also to the reaction that may lead to CNO^- formation. Therefore, we assume that reaction (4) is endothermic. Taking the electron affinity of our calculation of 0.26 eV and a threshold of 3 eV in Fig. 5, we get an estimate for the dissociation energy of 3.26 eV. Bearing in mind that the isotopic ratios for ^{16}O and ^{18}O are approximately 500:1, H_2NO^- signal could also be due to $^{14}N^{18}O^-$. However, we can discard this assumption since the cross-section shape and the resonance positions for both $^{14}N^{16}O^-$ and H_2NO^- are not identical.

4.7. NO^-

Formation of NO^-/CH_3NO_2 has been reported by Di Domenico and Franklin [1] and Sailer et al. [4]. Whereas Sailer et al. did not make any further analysis due to the very low intensity of the resonances, in Ref. [1] a main resonance at 8.3 eV together with two other plateau features at 4 and 6.5 eV, respectively, are reported, and interpreted as resulting from dissociative resonance capture. The DEA cross-section in Fig. 5 suggests the presence of three resonances at 4, 7 and 9 eV with an extra weak shoulder at ∼5.5 eV (Table 1). NO^- formation must proceed along the following reaction

$$e^- + CH_3NO_2 \rightarrow (CH_3NO_2)^{\#-} \rightarrow NO^- + CH_3 + O \qquad (5)$$

Taking the EA(NO) ∼3 eV, the $\Delta_f H_g{}^\circ(O) = 2.56$ eV, $\Delta_f H_g{}^\circ(CH_3) = 1.5$ eV and $\Delta_f H_g{}^\circ(CH_3NO_2) = -0.841 \pm 0.001$ eV [4], then $\Delta_f H_g{}^\circ(NO^-) = -1.93$ eV.

4.8. CN^-

The DEA cross-section for CN^-/CH_3NO_2 formation is shown in Fig. 4 and the estimated positions for the resonances are presented in Table 1 in good agreement with those reported before [4].

4.9. $^{16}O^-$, OH^- and $^{18}O^-$

DEA leading to the formation of $^{16}O^-$ and OH^- have been discussed previously [4] with the present high energy resonances (Fig. 4 and Table 1) in good agreement with those reported before. As far as the cross-section values for $^{18}O^-$ formation are concerned, the 6 and 9 eV resonances are within the expected isotopic ratio of 1:500 corresponding to the $^{16}O^-$ formation. In contrast to the measurements by Sailer et al. [4], OH^- does not show a detectable anion yield below 2 eV. The dominant narrow low-energy feature was attributed to vibrationally hot molecules [4]. In the present study nitromethane was also introduced at room temperature and thus we should also observe at least some signal close to 0 eV. One difference to [4] is the diameter of the gas capillary, i.e., a 20 μm nozzle in [4] and a 1 mm tube in the present study. The large pressure difference before and after the small nozzle utilized by Sailer at al. [4] may lead to the formation of a few neutral nitromethane clusters. OH^- formation upon DEA to such clusters could explain the 0 eV resonance observed in [4].

4.10. $CH_3{}^-$

$CH_3{}^-$ is a remarkable anion given the fact that the electron affinity of CH_3 is within the accuracy of the calculations 0 eV. An electronically excited state of the anion, however, might possess a high electron affinity and if its lifetime is in the range of a few μs which is the time window of the present experiment it could explain the presence of this fragment. Relaxation of such an electronically excited metastable state into the ground state and subsequent autodetachment can be measured with the present set-up in a short third field free region between the electrostatic sector field and a pair of deflector plates in front of the channeltron detector. Dressler and Allan [11] reported on autodetachment of $CH_3{}^-$ formed upon DEA to acetaldehyde. For nitromethane we also observe a metastable loss of the attached electron and obtain a lifetime of ∼820 μs for this anion. The partial cross-section for this anion is shown in Fig. 3. The reaction that leads to the methyl radical anion is complementary to that of $NO_2{}^-$ formation with respect to the negative charge. In Fig. 3 at least two high energy resonances at 7 and 8.5 eV (Table 1) can also be assigned to core excited resonances. The DEA cross-section above 12 eV rises which can be explained in terms of ion pair formation, bearing in mind that the $AE(NO_2{}^+) = 12.1$ eV [12].

4.11. $CH_2{}^-$

The present measurement for mass 14, shown in Fig. 3, reveals two relatively narrow resonances centred at ∼6 and 9.5 eV and a broad resonance at ∼13 eV. The appearance of a fragment ion with the composition of $CH_2{}^-$ (reaction (6)) is surprising due to the involvement of hydrogen transfer in the precursor ion and cleavage of the C–O bond. Bearing in mind that the $EA(CH_2) = 0.652 \pm 0.006$ eV [12], the $AE(CH_2{}^-) = D(H–CH_2NO_2) + D(CH_2–NO_2)–EA(CH_2)$ [8,9], the threshold for the appearance energy (AE) of $CH_2{}^-$ is estimated to be 5.3 eV which seems to be slightly higher than the value obtained in the present experiment for reaction

$$e^- + CH_3NO_2 \rightarrow (CH_3NO_2)^{\#-} \rightarrow CH_2{}^- + OH + NO \qquad (6)$$

If we take from Fig. 3 the $AE(CH_2{}^-)$ ∼4 eV, from Ref. [1] $\Delta_f H_g{}^\circ(NO) = 0.94$ eV and $\Delta_f H_g{}^\circ(OH) = 0.40$ eV, and $\Delta_f H_g{}^\circ(CH_3NO_2) = -0.841 \pm 0.001$ eV from [4], then $\Delta_f H_g{}^\circ(CH_2{}^-) = 3.5$ eV.

4.12. CH^-

The partial cross-section for the DEA reaction channel CH^-/CH_3NO_2 is shown in Fig. 3, with two major resonances at 6.0 and 9.5 eV (Table 1). However, a closer inspection of the 6.0 eV feature shows an asymmetric feature which may be due to the contribution of a low energy underlying resonance at ∼4.5 eV. Di Domenico and Franklin [1] have reported the presence of this anion at 5.6, and 8.2 eV and a weak contribution at ∼4 eV, in good agreement with the present DEA measurements. The reaction

$$e^- + CH_3NO_2 \rightarrow (CH_3NO_2)^{\#-} \rightarrow CH^- + H_2O + NO \qquad (7)$$

is endothermic with a threshold that can vary from 3.79 up to 4.71 eV if we take into account the values of $\Delta_f H_g{}^\circ(CH^-) = 4.52–5.44$ eV [1], $\Delta_f H_g{}^\circ(CH_3NO_2) = -0.841 \pm 0.001$ eV and $\Delta_f H_g{}^\circ(H_2O) = 2.51$ eV [4]. Therefore, the formation of CH^- ion at low electron energy around 3.5 eV seems to be energetically allowed as it may be for the other two resonances if we take into consideration the large uncertainties involved.

4.13. H^-

The partial cross-section for the DEA reaction channel H^-/CH_3NO_2 is shown in Fig. 3. H^- has been reported in the early experiment of Di Domenico and Franklin [1] but due to low intensity reasons, the ionic yields have not been shown. The spectrum shown in Fig. 3 represents the recorded H^- signal obtained by subtracting the background signal (with a pressure of 10^{-5} Pa) from the sample signal (at a working pressure of 10^{-3} Pa). The reaction

$$e^- + CH_3NO_2 \rightarrow (CH_3NO_2)^{\#-} \rightarrow CH_2NO_2 + H^- \qquad (8)$$

is complementary to (1) with respect to the negative charge. Taking from our calculation that $EA(H) = 0.75\,eV$ [13] and $D(CH_2NO_2\text{–}H) = 4.33\,eV$ (see Section 3), we obtain $AE(H^-) = 3.58\,eV$, which is below the observed threshold. With the value of $\Delta_f H_g{}^\circ(CH_2NO_2) = 0.87\,eV$ [1], we therefore obtain $\Delta_f H_g{}^\circ(H^-) = 2.09\,eV$. At energies in the vicinity of electronically excited states of the neutral molecule, fragmentation most likely originates from a core-excited resonance, consisting of two electrons in normally unoccupied MOs moving in the field of the positive core. The structures observed for H^- (7.5, 9.0 eV) (Fig. 3 and Table 1) are signatures of a core-excited resonance initiated via ($\sigma \rightarrow \pi^*$) or ($\pi \rightarrow \pi^*$) electron transitions [3]. The cross-section increases above 14 eV suggesting ion pair formation, which is reasonable since the $AE(CH_2NO_2{}^+) = 11.8\,eV$ [12].

5. Conclusions

The present DEA studies to nitromethane constitute a follow up to our earlier studies involving now a high mass resolution sector field mass spectrometer. The partial DEA cross sections have been measure with an electron energy resolution of ~1 eV in the electron energy range from about 0 to 16 eV. In addition to anions observed in previous studies, production of $CH_2NO_2{}^-$, $NOCH_2{}^-$, $NOH_2{}^-$ and H^- has been observed here. Formation of these anions at low electron energies, with the exception of H^-, has been explained by DEA to highly vibrationally excited molecules (hot bands). The high-energy resonances have been discussed as originating from core-excited resonances, consisting of two electrons in normally unoccupied molecular orbitals moving in the field of the positive core.

Acknowledgments

Work partially supported by the FWF, Wien. Some of this work forms part of the ESF network programme EIPAM and EU/ESF RADAM COST Action-P9. FFS and PLV acknowledge the RADAM COST-P9 support for the short-term scientific mission to Innsbruck.

References

[1] A. Di Domenico, J.L. Franklin, Int. J. Mass Spectrom. Ion Phys. 9 (1972) 171.
[2] A. Modelli, M. Venuti, Int. J. Mass Spectrom. 205 (2001) 7.
[3] I.C. Walker, M.A.D. Fluendy, Int. J. Mass Spectrom. 205 (2001) 171.
[4] W. Sailer, A. Pelc, S. Matejcik, E. Illenberger, P. Scheier, T.D. Märk, J. Chem. Phys. 117 (2002) 7989.
[5] R.N. Compton, H.S. Carman Jr., C. Desfrancois, H. Abdoul-Carime, J.P. Schermann, J.H. Hendricks, S.A. Lyapustina, K.H. Bowen, J. Chem. Phys. 105 (1996) 3472.
[6] T. Sommerfeld, Phys. Chem. Chem. Phys. 4 (2002) 2511.
[7] H.U. Poll, V. Grill, S. Matt, N. Abramzon, K. Becker, P. Scheier, T.D. Märk, Int. J. Mass Spectrom. Ion Processes 177 (1998) 143;
H.C. Straub, D. Lin, B.G. Lindsay, K.A. Smith, R.F. Stebbings, J. Chem. Phys. 106 (1997) 4430;
C. Tian, C.R. Vidal, J. Phys. B: At. Mol. Opt. Phys. 31 (1998) 895.
[8] M. Polasek, F. Turecek, J. Phys. Chem. A 105 (2001) 1371.
[9] E.C.M. Chen, N. Welk, E.S. Chen, W.E. Wentworth, J. Phys. Chem. A 103 (1999) 9072.
[10] W. Sailer, A. Pelc, M. Probst, J. Limtrakul, P. Scheier, E. Illenberger, T.D. Märk, Chem. Phys. Lett. 378 (2003) 250.
[11] R. Dressler, M. Allan, Chem. Phys. Lett. 118 (1985) 93.
[12] NIST Chemistry WebBook, http://www.nist.gov.
[13] K.R. Lykke, K.K. Murray, Phys. Rev. A 43 (1991) 6104.